ANALYZING MULTI-SENSOR DATA FUSION TECHNIQUES: A MULTI-TEMPORAL CHANGE DETECTION APPROACH

Chintan A. Shah
University of California Los Angeles, Los Angeles, CA
cashah@ucla.edu

Lindi J. Quackenbush, Assistant Professor
State University of New York – College of Environmental Science and Forestry, Syracuse, NY
ljquack@esf.edu

ABSTRACT

An inevitable tradeoff between spectral and spatial resolution exists in remote sensing systems and it is essential to integrate information from systems with complementary characteristics to improve data interpretability. Panchromatic (PAN) sharpening is a data fusion technique that merges a high spatial resolution PAN image with lower spatial resolution multispectral images. The resulting merged data, which inherits the spectral characteristics of the multispectral images, has the spatial resolution of the PAN image. This paper presents a comprehensive assessment of PAN sharpening techniques. Numerous studies have investigated the use of sharpening techniques for improved machine interpretability and evaluated the sharpening performance using univariate statistical measures. However, studies have not explored the interaction between sharpening and change detection. Since the ability to repeatedly acquire images over a specific ground area for detecting changes is sensor platform dependent, the significance of multi-sensor image change detection has increased in recent years. In fact, change detection can serve to be an effective measure for evaluating the performance of sharpening methods. By employing an image acquired in a spectral range most pertinent for detecting changes in a specific material; change detection can highlight the inefficiency of methods in sharpening individual images. Hence, the effect of sharpening on change detection is exploited in this paper and the experimental results underline the significance of change detection as an effective measure for evaluating the PAN sharpening methods.

INTRODUCTION

An inevitable tradeoff between spectral and spatial resolution exists in remote sensing systems. Spectral resolution is the ability to discriminate fine spectral differences, whereas spatial resolution defines the degree of spatial detail in an image. It is therefore essential to integrate fine spectral and spatial information from systems with complementary resolution characteristics to improve data interpretability. Panchromatic (PAN) sharpening is a data fusion technique that merges a high spatial resolution PAN image with lower spatial resolution multispectral images. The resulting merged data, which inherits the spectral characteristics of the multispectral images, has the spatial resolution of the PAN image. Techniques developed for PAN sharpening can be extended for band sharpening, which involves a high spatial resolution multispectral image instead of a PAN image. Derivatives of high spatial resolution multispectral images—e.g. Normalized Difference Vegetation Index (NDVI), texture, image ratio, principal component—can also substitute for a PAN image (Murdock et al., 2000).

This paper presents a comprehensive study of widely used PAN sharpening techniques. Vrabel (2000) provided a systematic evaluation of several sharpening techniques and demonstrated the improved visual interpretability of sharpened images in terms of their effective ground sampling distance (GSD). Numerous studies have investigated the use of sharpening techniques for improved machine interpretability and the sharpening performance was primarily evaluated using univariate statistical measures (Wald et al., 1997). Munechika et al. (1993) exploited the enhanced spectral and spatial information content of the sharpened images for classification. Thereafter, evaluating the influence of PAN sharpening on various post processing techniques such as classification, edge detection (Shen et al., 1994), material identification and anomaly detection (Shen, 2002) gained significant consideration. It also inspired the use of several multivariate statistical measures such as multivariate analysis of variance (MANOVA) and discriminant analysis, to determine the class separability in sharpened images (Murdock et al., 2000).

Studies, however, have not explored the interaction between sharpening and change detection. Since the ability to repeatedly acquire images over a specific ground area for detecting changes is sensor platform dependent, the significance of multi-sensor image change detection has increased in recent years. In fact, change detection can serve to be an effective measure for evaluating the performance of sharpening methods. Several studies (e.g., Wald et al., 1997) have reported that classification minimizes discrepancies between sharpening methods. This stems from the fact that sharpening methods exhibit comparable performances when the multispectral images are highly correlated with the PAN image. However, performance of many sharpening methods deteriorates for multispectral images that are uncorrelated with the PAN image. Most classification methods are robust to the effect of noise, which is caused by sharpening uncorrelated multispectral images. By employing an image acquired in a spectral range most pertinent for detecting changes in a specific material; change detection can highlight the inefficiency of methods in sharpening individual images. Hence, the effect of sharpening on change detection is exploited in this paper and the experimental results underline the significance of change detection as an effective measure for evaluating the PAN sharpening methods.

PAN SHARPENING METHODS FOR MACHINE INTERPRETATION

Sharpening methods may be broadly categorized based on their applicability for visual or machine interpretation. This paper primarily investigates sharpening methods that are applicable for machine interpretation. The majority of sharpening techniques make implicit assumptions regarding the superimposability of images at different spatial resolutions. This can be achieved by spatial resampling of the multispectral images, which are then registered with the PAN image. In this paper, sharpening methods based on pixel replication, high pass filtering (HPF) (Chavez et al., 1991), principal component analysis (PCA) (Chavez et al., 1991), and also those proposed by Pradines (1986), Price (1987), Shen et al. (1994), Zhang (1999), Ranchin and Wald (2000), and Winter and Winter (2002) are considered.

High Pass Filtering

The high pass filtering (HPF) sharpening technique (Chavez et al., 1991) extracts high frequency components from the PAN image using a high pass filter. These are then incorporated into low frequency components of the multispectral images, as given by the following equation,

$$S_{\lambda}(x,y) = \left\{ w_{high} \cdot \mathrm{HPF}\left[\mathrm{PAN}(x,y)\right] \right\} + \left\{ w_{low} \cdot \mathrm{LPF}\left[O'_{\lambda}(x,y)\right] \right\} \qquad (1)$$

to generate the corresponding sharpened images. In equation (1), $\mathrm{PAN}(x,y)$ and $O'_{\lambda}(x,y)$ correspond to a pixel at location (x,y) in the PAN image and the interpolated and registered multispectral image (at wavelength λ), respectively. $\mathrm{HPF}[\bullet]$ and $\mathrm{LPF}[\bullet]$ correspond to the high and low pass filter operators, respectively. The result after applying the filter operator on an image I at location (x,y) can be expressed as $\sum_{j=-k_y}^{k_y} \sum_{i=-k_x}^{k_x} \left[w_{i,j} \cdot I(x+i, y+j) \right]$. Here, k_x and k_y are related to the kernel size N_x and N_y along the x and the y axis as $k_x = \frac{N_x + 1}{2}$ and $k_y = \frac{N_y + 1}{2}$, whereas $w_{i,j}$ are the filter coefficients. The frequency components are combined in a proportion determined by the corresponding weighting coefficients w_{high} and w_{low}. The high frequency components can be related to the spatial information in an image, whereas the low frequency components correspond to the spectral information. Factors that influence the performance of this technique are filter coefficients ($w_{i,j}$) and window size (N_x and N_y), in addition to weights (w_{high} and w_{low}) that determine the amount of frequency components being combined.

Principal Component Analysis Sharpening

Principal component analysis (PCA) is a linear orthogonal transformation that projects the multivariate data on a subspace spanned by the principal axes. Thus, the principal components are obtained by projecting the multispectral images on the principal axes (eigenvectors) estimated from the sample covariance matrix. The first principal component exhibits the highest data variance. In PCA-based sharpening (Chavez et al., 1991), the PAN image replaces the first principal component, before an inverse principal component transform is performed. Prior to substitution, the PAN image is stretched such that its mean and variance are similar to that of the first principal component.

Pradines Approach to Sharpening

Pradines (1986) proposed an approach for merging the multispectral images that are strongly correlated with the PAN image. The merged pixel is estimated as

$$S_{\lambda}\left(x,y\right)=O'_{\lambda}\left(x,y\right)\cdot\left[\frac{\mathrm{PAN}\left(x,y\right)}{\sum_{v\in n_y}\sum_{u\in n_x}\mathrm{PAN}\left(u,v\right)}\right] \qquad (2)$$

In equation (2), n_x and n_y correspond to the neighborhood of x and y, respectively, such that it consists of the PAN image pixels that are encompassed by the original multispectral image pixel. As an example, when merging the SPOT PAN image with the multispectral SPOT-1 XS images, each pixel in the multispectral image (GSD 20 m) encompasses the 4 PAN image pixels (GSD 10 m) in its 2 × 2 neighborhood (Pradines, 1986). The sharpened image is thus a product of the resampled multispectral image pixel with a ratio of corresponding PAN image pixel and the sum of PAN image pixels that are encompassed by a low spatial resolution multispectral image pixel.

Price Approach to Sharpening

Price (1987) proposed a two-stage sharpening algorithm to effectively sharpen multispectral images that are uncorrelated with the PAN image. The first stage sharpens the multispectral images (that are correlated with the PAN image) by assuming a linear relation between the PAN image and the multispectral images and estimates the least squares coefficients a_{λ} and b_{λ} such that,

$$O_{\lambda}\left(x,y\right)=\left[a_{\lambda}\cdot\mathrm{PAN}_{Avg}\left(x,y\right)\right]+b_{\lambda}. \qquad (3)$$

In equation (3), $\mathrm{PAN}_{Avg}\left(x,y\right)=\frac{1}{T}\cdot\left[\sum_{v\in n_y}\sum_{u\in n_x}\mathrm{PAN}\left(u,v\right)\right]$, where T is the total number of PAN image pixels encompassed by the corresponding multispectral image pixel. The least square coefficients are subsequently employed for estimating the merged pixel as,

$$S_{\lambda}\left(x,y\right)=O'_{\lambda}\cdot\left[\frac{\tilde{O}_{\lambda}}{\tilde{O}_{\lambda(Avg)}}\right]. \qquad (4)$$

where $\tilde{O}_{\lambda}=\left[a_{\lambda}\cdot\mathrm{PAN}\left(x,y\right)\right]+b_{\lambda}$. Equation (4) is similar to the equation (2) for Pradines' method with the exception that Price uses an estimate of a multispectral image instead of the PAN image for the sharpening process. In the second stage, prior to sharpening the multispectral images that are uncorrelated with the PAN images, a look up table (LUT) is employed to transform the PAN image in order to establish a relation with the multispectral image.

Shen Approach to Sharpening

Shen et al. (1994) utilized a method similar to that of Price for sharpening multispectral images that are correlated with the PAN image. However, for sharpening uncorrelated multispectral images, Shen et al. employs an average preserving filter, which estimates the sharpened image pixel as,

$$S_{\lambda}(x,y) = O'_{\lambda} \cdot \left[\frac{\mathrm{PAN}(x,y)}{\mathrm{PAN}_{Avg}(x,y)} \right]. \qquad (5)$$

In equation (5), the ratio within the parenthesis is termed as the average preserving filter.

Synthetic Variable Ratio based Sharpening

Based on an atmospheric model, Munechika et al. (1993) proposed a synthetic variable ratio (SVR) merging method that was superior to the methods proposed by Pradines and Price. However, due to its limitations in estimating the parameters from specific land cover classes, Zhang (1999) extended this method by estimating the required parameters through multiple regression analysis.

Wavelet-based Sharpening Approaches

Through the ARSIS concept for sharpening SPOT images, Ranchin and Wald (2000) introduced a multi-scale sharpening technique that employed a wavelet transform. It performed sharpening by extracting missing spatial information between multispectral image and the PAN image. Currently, research efforts are being directed in developing sharpening techniques based on 'algorithm fusion'. For example, a PCA-Wavelet approach proposed by Winter and Winter (2002) overcomes the limitations of each of the individual methods (PCA and Wavelet) in sharpening the multispectral images.

EVALUATION OF SHARPENING METHODS

Literature has revealed successful application of the aforementioned techniques and their variants for sharpening the images acquired by multispectral and hyperspectral sensors, with varying sharpening ratios. However, few efforts have been made in comparing the sharpening performances of such methods. This can primarily be attributed to unavailability of a suitable reference image, an image acquired by the multispectral sensor with spatial resolution equal to that of the PAN image. It is interesting to note that in the case where spatially degraded multispectral images are sharpened, the sharpening quality, even in the presence of the reference multispectral images, defies a precise definition (Wald et al., 1997; Chavez et al., 1991; Alparone et al., 2004). In our work, we categorize the measures for quantitative evaluation of the performance of the sharpening algorithm as either 'statistical' or 'application oriented'. Statistical measures quantify the spectral distortion introduced by the sharpening process; whereas application oriented measures evaluate the impact of sharpening on the post-processing algorithm employed for a specific application. In the following discussion, we provide a detailed description of the various measures in each of these categories.

Wald et al. (1997) presented several widely accepted criteria for quantitative assessment of sharpening methods. These criteria were chosen to test three particular properties. First, when degraded back to the original spatial resolution the sharpened image should be identical to the low spatial resolution image. This property ensures that the sharpening process does not alter the spectral properties of the multispectral images. Second, the sharpened image should be identical to the image that would be acquired by the multispectral sensor with spatial resolution equal to that of the PAN image. Various statistical measures employed to test these two properties are root mean square error (RMSE), mean and relative mean, variance and relative variance, correlation coefficient, and entropy. Finally, the sharpened multispectral images should have correlation coefficients identical to that of the multispectral images that would be acquired by the sensor with spatial resolution equal to that of the PAN image.

In contrast to the statistical measures, which are application independent, application oriented methods evaluate the sharpening performance by taking into consideration the particular application for which the sharpened images are employed. The sharpening performance is quantified by the accuracy of the post-processing algorithm applied on the sharpened images, thus eliminating the need for a sharpened reference. The influence of PAN sharpening on

class separability (Murdock et al, 2000) and post processing techniques such as classification (Munechika et al. 1993), edge detection (Shen et al., 1994), material identification and anomaly detection (Shen, 2002) has been investigated by several researchers.

Many of the above mentioned measures have been employed in this paper to evaluate the performances of sharpening methods. In addition, an evaluation of sharpening methods based on their impact on change detection is proposed in this paper. Statistical hypothesis testing for change detection consists of selecting one of the two competing hypothesis (Kay, 1998); the null hypothesis $\mathcal{H}_0$ indicating no change or the alternative hypothesis $\mathcal{H}_1$ that corresponds to change. Let $P(\mathcal{H}_i;\mathcal{H}_j)$ denote the probability of deciding $\mathcal{H}_i$ when $\mathcal{H}_j$ is true, then $P(\mathcal{H}_1;\mathcal{H}_0)$ the probability of declaring an 'unchanged' pixel as 'changed' is referred as the probability of false alarm (P_{fa}). Hence, to design an optimal detector one seeks to maximize $1-P(\mathcal{H}_0;\mathcal{H}_1)$, which is just $P(\mathcal{H}_1;\mathcal{H}_1)$ and in keeping with the signal detection problem it is called the probability of detection (P_d). Change detection performance is thus quantified by P_d and P_{fa}. A receiver-operating-characteristic (ROC) curve provides graphical representation of P_d versus P_{fa} for binary hypothesis testing as its discrimination threshold is varied.

EXPERIMENTS

Multispectral IKONOS imagery (blue: 0.45-0.52 μm, green: 0.52-0.60 μm, red: 0.63-0.69 μm and near IR: 0.76-0.90 μm) acquired in August 2001 over the Syracuse area was used in this study. The data was provided by the Mapping Sciences Laboratory at the State University of New York, College of Environmental Science and Forestry. The objective of this experiment was to study the performance of various methods for a multispectral image to PAN sharpening ratio of 30:1. Similar to the approach proposed in Vrabel (2000), a PAN image (0.45-0.69μm) with 4m spatial resolution is simulated by averaging the multispectral images of IKONOS in the visible wavelength. Multispectral images of 120m spatial resolution are obtained by spatially degrading the high spatial resolution multispectral IKONOS images using a spatial averaging filter.

In the following discussion, the terms "reference" and "sharpened" are used for the high spatial resolution multispectral images and sharpened multispectral images, respectively, whereas the simulated multispectral images are referred to as the "original" multispectral images. Thus, the reference images in this context correspond to the initial multispectral IKONOS images with a pixel size of 4 m, whereas these images down sampled by a factor of 30 lead to the generation of the original images with a pixel of 120 m. The down sampling involved averaging pixel values within a 30 × 30 window in the 4 m GSD reference image to form each pixel in the lower resolution simulated image.

Prior to sharpening, the simulated multispectral images need to be superimposed on the high spatial resolution PAN image. This constitutes interpolating (up sampling) the original images, followed by registration to the PAN image. At this point, one can comprehend the benefit of also simulating the PAN image, thus eliminating the need for performing spatial registration. Though registration of multi-sensor (as well as multi-resolution) images is an explored issue (e.g. Fonesca and Manjunath, 1996), the registration process itself introduces errors (Bruzzone and Cossu, 2003), which can further influence the performance of sharpening. As recommended by Chavez et al. (1991), bi-cubic interpolation was employed in order to limit the artifacts caused by resampling.

Statistical Analysis of Sharpened Images

For convenience, the abbreviated names of the various sharpening algorithms employed in the experiments are given in Table 1.

The replication method (Rep) for sharpening is the most primitive sharpening technique. As the name suggests, this technique replicates each pixel in the original image in order to generate an image with smaller pixel size. Thus, each pixel in the 120 m simulated image is replicated 30 × 30 times to form a 4 m sharpened image. This method does not use the PAN image and is unsuitable for practical applications. However, we have included this approach in our comparison in order to highlight the differences between the process of sharpening and interpolation. The latter estimates the values of 'missing pixels' based on the existing pixels in that image, thus rendering the process

independent of the PAN image. Also, by comparing the sharpening performance (through statistical or application oriented measures) of the replication method, we can identify the improvement in sharpening achievable by each of the sharpening algorithms that employ the PAN image.

Table 1. Abbreviations for sharpening methods considered in experimentation

Sharpening Method	Abbreviation
Replication method for sharpening	*Rep*
High Pass Filtering method for sharpening	*HPF*
PCA method for sharpening	*PCA*
Sharpening method proposed by Pradines	*Prad*
Sharpening method proposed by Price	*Price*
Sharpening method proposed by Shen *et* al.	*Shen*
Wavelet method for sharpening	*Wav*
Sharpening method proposed by Zhang	*Zhang*
PCA-Wavelet method for sharpening	*PCWav*

The HPF method for sharpening extracted the high frequency components of the PAN image using a high pass filter of window size 3 × 3 and extracted the low frequency components of the multispectral image, using a 3 × 3 low pass filter. These two components were then combined. Based on experimentation with the given dataset, the weighting coefficients shown in equation 1, w_{high} and w_{low}, were chosen to be 0.2 and 0.8, respectively. The normalized eigenvalues as estimated from the covariance matrix of the given multispectral data are 0.7125, 0.2851, 0.0023, and 0.0001. Hence, it can be noticed that the first principal component for the PCA method exhibits significantly high data variance.

As discussed in the earlier Section, the statistical measures employed in this paper are percent relative mean (RM), percent relative variance (RV), correlation coefficient (CC), relative entropy (RE), and root mean square error (ER). A detailed description of each of these statistical measures can be obtained from Wald et al. (1997). Relative entropy, also known as Kullback-Leibler (KL) divergence, measures the distance between two probability distributions. The lower the RE value, the higher the mutual information between the sharpened and reference images. Table 2(a)-(d) provide the statistical measures that illustrate discrepancies between the sharpened and the reference images in blue, green, red, and NIR wavelengths, respectively.

Table 2. Statistical measures depicting discrepancies between the sharpened and the reference images (a) Blue: 0.45-0.52μm, (b) Green: 0.52-0.60μm, (c) Red: 0.63-0.69μm, and (d) Near IR: 0.76-0.90μm

SM	Sharpening Method								
	Rep	HPF	PCA	Prad	Price	Shen	Wav	Zhang	PCWav
RM	0	-1.79	32.58	99.89	0	0	98.58	33.09	15.92
RV	63.09	-30.59	70.72	100	-5.86	-5.86	$-8.8\text{x}10^4$	32.21	-53.69
CC	0.61	0.67	0.89	0.90	0.91	0.91	0.13	0.91	0.60
RE	0.08	14.71	1.26	1.37	1.11	1.11	9.83	0.90	14.65
ER	92.50	102.62	132.46	368.68	50.58	50.58	$3.4\text{x}10^4$	125.99	131.96

(a)

SM	Sharpening Method								
	Rep	HPF	PCA	Prad	Price	Shen	Wav	Zhang	PCWav
RM	0	-1.33	41.57	99.89	0	0	98.17	32.90	20.26
RV	65.58	17.97	72.52	100	33.13	33.13	$-3\text{x}10^4$	49.57	-44.45
CC	0.59	0.74	0.92	0.94	0.93	0.93	0.12	0.94	0.65
RE	0.27	11.97	0.14	0.03	0.11	0.11	8.27	0.05	12.10
ER	127.37	108.07	173.00	391.41	59.44	59.44	$2.6\text{x}10^4$	135.19	163.77

(b)

SM	Sharpening Method								
	Rep	HPF	PCA	Prad	Price	Shen	Wav	Zhang	PCWav
RM	0	-8.56	55.02	99.89	0	0	98.76	32.67	26.77
RV	66.55	20.23	73.56	100	49.53	49.53	$-2.7x10^4$	60.82	-38.86
CC	0.58	0.74	0.91	0.92	0.89	0.89	0.11	0.91	0.65
RE	0.09	12.20	0.35	0.04	0.34	0.34	9.13	0.20	12.40
ER	130.07	113.35	173.97	312.45	79.02	79.02	$2.6x10^4$	119.04	164.27

(c)

SM	Sharpening Method								
	Rep	HPF	PCA	Prad	Price	Shen	Wav	Zhang	PCWav
RM	0	5.20	4.84	99.89	0	0	97.77	32.79	2.01
RV	81.88	64.81	83.91	100	80.57	46.23	$-3.8x10^4$	73.62	82.36
CC	0.43	0.70	0.51	0.45	0.62	0.78	0.05	0.76	0.60
RE	1.46	5.64	1.59	2.96	1.22	1.04	7.03	2.66	2.49
ER	213.31	171.63	205.97	584.08	210.67	147.87	$1.5 x10^4$	240.08	193.83

(d)

The replication, Price and Shen methods have an ideal relative mean of zero for all the four multispectral bands. Both the relative mean and relative variance indicate the quantity of information added (-ve) or eliminated (+ve) during the sharpening process. As in the case of Wavelet method, the negative RVs indicate that there was too much 'innovation' in the sharpened images. This renders such methods inefficient for sharpening the images to be employed for machine interpretation. Table 2(a)-(c) also show that for the visible bands, which are highly correlated with the PAN band, PCA, Prad, Price, Shen, and Zhang methods exhibit comparable correlation coefficients. Shen's superiority in sharpening the uncorrelated near-IR image is confirmed through its relatively high CC of 0.78 shown in Table 2(d). Due to their similarity in processing multispectral images that are correlated with the PAN image, Price and Shen lead to identical results. The inability of Pradine's method in sharpening uncorrelated data is verified from its statistical measures shown in Table 2(d). The lowest ER of all the Shen sharpened MSI indicates its increased applicability for machine interpretation.

Table 3 provides the correlation coefficients of the PAN and simulated multispectral image with the sharpened multispectral image to verify the third criterion for quantitative assessment. According to the third criterion, the sharpened multispectral images should have correlation coefficients identical to that of the multispectral images that would be acquired by the sensor with spatial resolution equal to that of the PAN image. In Table 3, the Reference column corresponds to the correlation coefficients of the PAN image with the high spatial resolution multispectral images. Whereas, the remaining columns depict the correlation coefficients of the PAN image with the multispectral images sharpened using the corresponding sharpening techniques. The values indicate that the high spatial resolution NIR image has a low correlation with the PAN image due to the fact that the PAN image was simulated by averaging the bands in the visible range only. PCA, Prad, Price, Shen, and Zhang methods lead to significantly high correlation between the sharpened images in the visible range and the PAN image. Interestingly, only Prad, Shen, and Zhang methods retain high correlation of the sharpened NIR with the PAN image. Furthermore, the Wav method shows very high correlation between NIR and each of the visible bands.

Table 3. Correlation coefficient for PAN - MSI and MSI - MSI.

		Sharpening Method								
Images	Reference	Rep	HPF	PCA	Prad	Price	Shen	Wav	Zhang	PCWav
Pan-blue	0.87	0.49	0.80	0.99	0.98	0.97	0.97	0.12	0.97	0.75
Pan-green	0.91	0.50	0.81	0.99	0.97	0.94	0.94	0.12	0.96	0.76
Pan-red	0.90	0.50	0.81	0.99	0.95	0.88	0.88	0.12	0.93	0.76
Pan-NIR	0.64	0.25	0.70	0.61	0.82	0.29	0.82	0.12	0.88	0.45
blue-green	0.98	0.99	0.99	0.99	0.99	0.98	0.98	0.99	0.99	0.99
blue-red	0.95	0.99	0.99	0.99	0.97	0.93	0.93	0.99	0.98	0.99
blue-NIR	0.20	0.11	0.79	0.23	0.69	0.11	0.67	0.94	0.76	0.37
Green-red	0.97	0.99	0.99	0.99	0.99	0.98	0.98	0.99	0.99	0.99
Green-NIR	0.27	0.16	0.77	0.28	0.67	0.16	0.60	0.94	0.73	0.39
red-NIR	0.25	0.14	0.77	0.26	0.60	0.15	0.49	0.95	0.67	0.38

Classification of Sharpened Images

Through visual analysis of the reference multispectral image and using the 1 m IKONOS panchromatic band, 1000 training and 1000 testing pixels were identified for each of the four classes: (a) Roof top, (b) Roads, (c) Low vegetation, and (d) Trees. Table 4 depicts the Overall, User's, and Producer's accuracy obtained by classifying the sharpened multispectral image using a supervised maximum likelihood classification (MLC).

Table 4. Classification Accuracies

Class	Reference	Sharpening Method								
		Rep	HPF	PCA	Prad	Price	Shen	Wav	Zhang	PCWav
Overall Accuracy (%)										
	90.5	90.0	91.7	94.0	86.5	86.6	87.9	44.9	91.8	90.5
Producers Accuracy (%)										
Roof top	78.5	89.6	92.5	87.5	89.7	90.2	91.5	73.9	93.9	76.6
Roads	93.8	86.4	91.0	92.8	92.8	91.6	91.8	66.9	93.6	93.5
Low veg.	94.6	87.9	96.4	98.6	85.8	86.5	87.1	24.2	93.7	97.2
Tree	94.9	96.1	86.8	97.2	77.5	78.1	81.0	14.8	86.0	94.9
Users Accuracy (%)										
Roof top	92.5	93.1	92.1	95.1	94.4	93.2	94.8	86.0	94.4	92.7
Roads	81.4	78.8	82.2	91.2	74.1	74.2	73.9	34.0	89.3	83.8
Low veg.	94.5	94.4	95.4	92.1	87.6	91.1	92.3	36.0	91.1	89.4
Tree	95.1	95.0	98.7	98.0	94.7	92.1	95.5	29.5	92.6	97.7

It is interesting to note that the Overall accuracy of the sharpened image is higher than that of the reference image in the case of PCA, Zhang and HPF. The maximum Overall accuracy of 94% for PCA can be attributed to its assertion of property three as identified from Table 3. Significantly higher performance in classifying spectrally similar classes—e.g. low vegetation and trees—highlights the increased class separability attainable though PCA.

Change Detection using Sharpened Images

The changed MSI ("changed reference") were simulated from the reference MSI by replacing pixels (training - 1000 and testing - 1000) in Low vegetation class by pixels in Tree class. Since the objective is to evaluate performance of the methods in sharpening the MSI uncorrelated with PAN (near-IR in this study) through change detection, changes were introduced specifically in vegetation class. The "changed original" MSI was obtained by degrading the changed reference MSI using an averaging spatial filter. Independent and identically distributed Gaussian noise with zero mean was added to the changed original MSI, resulting in 10dB SNR. Since many studies have proved Pradine's algorithm to be inefficient in sharpening uncorrelated images (also verified by the results shown in Table 2(d)), this method was not considered for this experiment.

The changes were detected using an image-differencing method. For varying thresholds, the Receiver Operating Characteristic plot in Figure 1 presents the corresponding P_d and P_{fa} respectively. Relatively high probability of detection (P_d ~1) for the reference image, at relatively low probability of false alarm (P_{fa}), contrasts the classification results in Table 4 where the sharpened image led to higher classification accuracy than the reference image. Shen's algorithm exhibits very high performance in detecting changes. It can also be noted that the change detection performance in Figure 1 can be ranked in accordance with the ER values in Table 2(d).

CONCLUSIONS

A comprehensive study of widely used PAN sharpening methods is presented in this paper. The statistical measures revealed superiority of Shen's method in sharpening multispectral imagery. When classified with a maximum likelihood classifier, the PCA sharpened imagery generated the highest classification accuracy. The ability of a sharpening method to retain correlation between the reference high spatial multispectral images and the sharpened images is shown to be a dominating factor in determining the classification accuracy. The proposed change detection based evaluation revealed the underlying relation between root mean square error (ER) and P_d. Owing to its high sensitivity to the sharpening of individual images; this approach is more suitable over the classification approach for evaluating the sharpening methods.

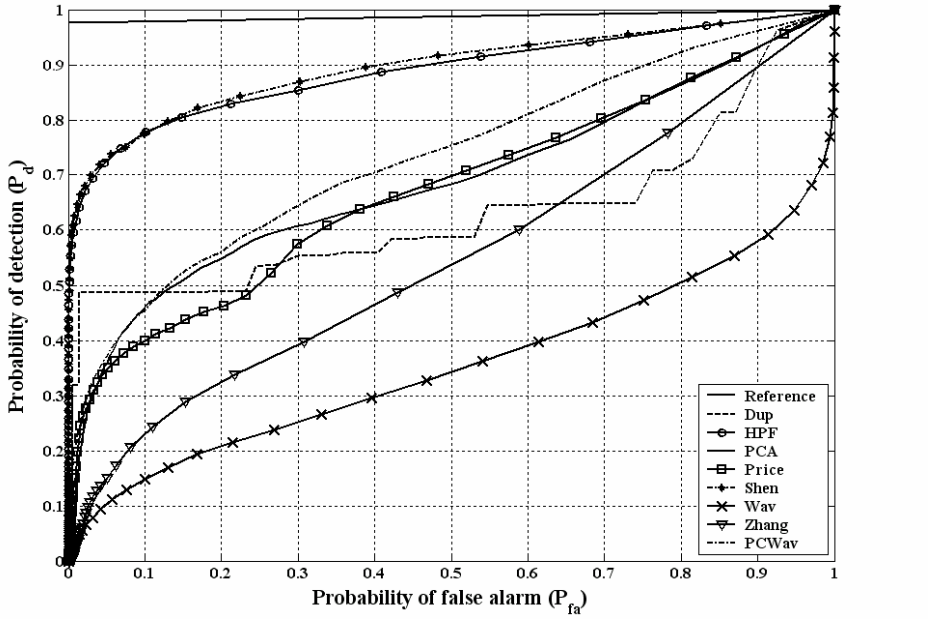

Figure 1. Receiver Operating Characteristic (ROC) curve for change detection.

REFERENCES

Alparone, L., S. Baronti, A. Garzelli, and F. Nencini, 2004. A global quality measurement of pan-sharpened multispectral imagery. *IEEE Geoscience and Remote Sensing Letter*, 1(4): 313-317.

Bruzzone, L., and R. Cossu, 2003. An adaptive approach to reducing registration noise effects in unsupervised change detection. *IEEE Transactions on Geoscience and Remote Sensing*, 41(6): 2455-2465.

Chavez, P. S. Jr., G. L. Berlin and L. B. Sowers, 1982. Statistical methods for selecting Landsat MSS ratios. *Journal of Applied Photographic Engineering*, 8(1): 23- 30.

Chavez, P. S. Jr., Sides, S. C., and Anderson, J. A., 1991, Comparison of three different methods to merge multiresolution and multispectral data: Landsat TM and SPOT panchromatic. *Photogrammetric Engineering and Remote Sensing*, 57(3): 295-303.

Fonesca, L. M. G. and Manjunath, B. S., 1996, Registration techniques for multisensor remotely sensed imagery. *Photogrammetric Engineering and Remote Sensing*, 62(9), 1049-1056.

Kay, S. M., 1998, Fundamentals of Statistical Signal Processing Volume 2: Detection Theory. *Prentice Hall PTR*, 1st edition.

Murdock, D., Riordan, K., and Quackenbush, L., 2000, Analysis of fusion techniques for forestry applications. Final Report.

Munechika, C. K., Warnick, J. S., Salvaggio, C., and Schott, J. R., 1993, Resolution enhancement of multispectral image data to improve classification accuracy. *Photogrammetric Engineering and Remote Sensing*, 59(1), 67-72.

Pohl, C., and Van Genderen, J. L., 1998, Multisensor image fusion in remote sensing: concepts, methods and applications. *International Journal of Remote Sensing*, 19(5), 823-854.

Pradines, D., 1986, Improving SPOT image size and multispectral resolution. *Proceedings SPIE Conference 'Earth Remote Sensing using the Landsat Thematic Mapper and SPOT Systems'*, 660, 78-102.

Price, J. C., 1987, Combining panchromatic and multispectral imagery from dual resolution satellite instruments. *Remote Sensing of Environment*, 21(2), 119-128.

Ranchin, T., and Wald, L., 2000, Fusion of high spatial and spectral resolution images: the ARSIS concept and its implementation. *Photogrammetric Engineering and Remote Sensing*, 66(1), 49-61.

Shen, S. S., Lindgren, J. E., and Payton, P. M., 1994, Panchromatic band sharpening of multispectral image data to improve machine exploitation accuracy. *Proceedings of the SPIE - The International Society for Optical Engineering*, 2304, 124-131.

Shen, S. S., 2002, Effects of sharpening on hyperspectral exploitation. *Proceedings of the SPIE - The International Society for Optical Engineering*, 4725, 568-579.

Thomas Carper, W., Lillesand, T. M., and Kiefer, R. W., 1990, The use of intensity-hue-saturation transformations for merging SPOT panchromatic and multispectral image data. *Photogrammetric Engineering and Remote Sensing*, 56(4), 459-467.

Vrabel, J., 2000, Multispectral imagery advanced band sharpening study. *Photogrammetric Engineering and Remote Sensing*, 66(1), 73-79.

Wald, L., Ranchin, T., and Mangolini, M., 1997, Fusion of satellite images of different spatial resolutions: assessing the quality of resulting images. *Photogrammetric Engineering and Remote Sensing*, 63(6), 691-699.

Winter, M. E., and Winter, E. M., 2002, Resolution enhancement of hyperspectral data. *IEEE Aerospace Conference Proceedings*, 3, 1523-1529.

Zhang, Y., 1999, A new merging method and its spectral and spatial effects. *International Journal of Remote Sensing*, 20(10), 2003-2014.